ROYAL SOCIETY OF CHEMISTRY

PAPER

Check for updates

Biofilm development, dynamics, and control in a pilot drinking water network with different pipe materials

Noora Salonen, [iD] *[a] Kalle Salonen,[a] Marko Suokas[b] and Martti Latva[a]

Biofilms in premise plumbing systems can decrease the quality of drinking water in several ways. Biofilm removal is possible utilizing disinfectants combined with mechanical cleaning, which can be expensive and challenging to implement in plumbing systems. Thus, alternative methods to control biofilms are needed. This study investigated the effects of hydrodynamic cavitation (HC) and magnetic water treatment (MWT), both of which produce nanobubbles, on biofilms in a pilot-scale drinking water network over a 16-month study period. Additionally, the influence of various materials, including copper, stainless steel, and PEX, on biofilms was investigated. A new biofilm-removal tool was developed to detach biofilms from pipes quantitatively. Biofilms were analyzed quantitatively and qualitatively. PEX promoted significantly higher biofilm growth than metallic materials throughout the sampling period. HC and MWT showed slight effects on biofilm growth in PEX pipes, enhancing growth in young biofilms and inhibiting growth in older biofilms. Biofilm quantities varied across time points due to seasonal fluctuations in water temperature, highlighting the dynamic nature of biofilms. According to the sequencing analysis, pipe material was the most significant factor affecting microbial communities. This study provides insight into the effects of various materials and nanobubble-generating treatments on biofilm growth in premise plumbing drinking water pipes. Due to the many variables and multiple effects caused by HC and MWT, further research is still required to understand the impact of nanobubbles on biofilm control.

Water impact

Premise plumbing biofilms significantly influence drinking water quality and stability. This study demonstrates how pipe material selection and two nanobubble-generating technologies—magnetic water treatment and hydrodynamic cavitation—affect biofilm accumulation. Results from a pilot-scale drinking water network, supported by a novel biofilm-removal tool, provide practical information for technology and material choices for water systems.

Introduction

Access to safe and clean drinking water is essential for the well-being of individuals and societies. Drinking water of sufficient quality does not pose health hazards in the form of harmful chemicals or harmful microorganisms. Drinking water delivered from waterworks is not sterile and contains various microbes depending on the water source and treatments. Microbes in water systems tend to attach to all moist surfaces, forming a biofilm—a slimy matrix composed of bacteria, extracellular polysaccharides, and other organic and inorganic materials. Biofilms serve as a natural habitat for bacteria and other microbes, where many species interact with each other and are better protected from changing environmental conditions. Biofilms inhabiting pipe and water fixture surfaces in premise plumbing are critical to water quality.[1]

Biofilm formation in premise plumbing systems can impair pipe materials, leading to corrosion and the dissolution of harmful substances. Additionally, biofilms can compromise the microbiological quality of drinking water, posing potential health risks, particularly for individuals with weakened immune systems. Premise plumbing biofilms can form a reservoir for opportunistic pathogens that is difficult to destroy. In favorable conditions, such as increased cold-water temperatures, low hot-water temperatures, and stagnation, microbes residing in biofilms begin to proliferate freely in the water, thereby reducing the microbiological quality of drinking water. In addition, pressure changes can release biofilms into drinking water. Maintaining the

[a] Research Center WANDER, Faculty of Technology, Satakunta University of Applied Sciences, Rauma, Finland. E-mail: noora.salonen@samk.fi
[b] Biocenter Oulu & Ecology and Genetics Unit, University of Oulu, Oulu, Finland

drinking water quality in premise plumbing typically aims to minimize the proliferation of microbes in water. The measures include ensuring the proper temperatures of hot and cold lines, maintaining the flow, and preventing stagnation and water aging.[2] Typically, drinking water leaving the waterworks is disinfected, such as through chlorination, to control microbial growth in the distribution network and premise plumbing. However, the residual disinfectant level may be low in premise plumbing, especially in the case of stagnation. In addition, microbes residing in biofilms can be 100 to 1000 times better protected against disinfectants than planktonic microbes.[3] Thus, disinfection can only control the microbial growth in biofilms within limits.[4] Effective biofilm removal from premise plumbing would typically require harsh disinfectants and mechanical cleaning. On the other hand, increased chlorine concentration in drinking water would have undesirable effects, such as increased corrosion of materials.[5] Moreover, harmful disinfection by-products can pose health risks, such as increasing the risk of, *e.g.*, cancer.[6] Additionally, disinfected water can lead to alterations in gut microbiota, resulting in dysbiosis.[7,8] Chlorine can also enhance the selection of antimicrobial-resistant bacteria.[9] Indeed, new, preferably additive-free approaches to control biofilms are desired.[10]

Nanobubbles have recently garnered significant attention in research and have been investigated for numerous applications. Nanobubbles are ultrafine bubbles with a diameter of less than 1 μm, typically 50–200 nm. They are present in nature and can be found in bulk liquid and on surfaces, but can also be generated artificially.[11] Nanobubbles have unique characteristics, such as negative surface charge, hydrophobic nature, long-term stability in solution, dominant Brownian motion, and theoretically high internal pressure, which may promote specific physicochemical processes, such as enhanced adsorption, hydrophobic interactions, reactive oxygen species (ROS) formation, and gas–liquid mass transfer.[12–14] These properties have opened up opportunities in numerous applications, such as water and wastewater treatment, environmental remediation, surface defouling, fermentation, and promoting the growth of crops.[11,15–17]

Nanobubbles have demonstrated antimicrobial and antifouling properties, but the mechanisms of action are partially unclear. It has been suggested that nanobubbles inactivate microorganisms by producing localized high temperatures, pressures, and hydroxyl radicals with strong oxidation activities during self-collapse. The vibrational motion of nanobubbles could cause shear stress, disrupting biofilms.[13] Hydroxyl radicals have high reactivity with organic matter, which enables their potential to remove organic matter, such as exopolysaccharides in the biofilm matrix.[18] The effects of nanobubbles on microbes supposedly depend on prevailing conditions, microbial species, and the identity of the gas. However, studies on biofilm mitigation utilizing nanobubbles in plumbing systems are scarce.

Xiao *et al.* investigated the impact of nanobubbles in an agricultural water distribution system, where nanobubbles effectively reduced the fixed biomass, biodiversity, and mineral deposits in irrigation pipes.[19] Nanobubbles were proposed to control biofilm formation directly by affecting microbes, and indirectly, by influencing water quality. Reducing microbial diversity would disrupt the mutual relationships between microbes, thereby destabilizing the biofilm structure. Additionally, nanobubbles are expected to reduce mineralization directly through chelation and suspension effects, and indirectly through the reduction of biofilms.[19] Luo *et al.* reported that oxygen nanobubbles caused a 78% reduction in biofilm dry weight during slow and rapid phases of biofilm growth (0–27 days and 27–42 days, respectively) in a biofilm reactor.[20] Nanobubbles have also been used to enhance the removal of biofilms from food processing surfaces.[18,21]

Nanobubbles can be prepared artificially, for example, by dissolving gas under high pressure and releasing it when the pressure is reduced, or by dispersing gas utilizing pressure changes in a flowing fluid. This phenomenon is known as hydrodynamic cavitation.[11,22] HC can create nanobubbles without bringing additional gas to the system. It can be applied to flowing water, *e.g.*, by integrating a nozzle with a specific internal structure that creates forces when changing the flow pattern and pressure. Nanobubble water generated in this manner has demonstrated high antimicrobial activity against *Escherichia coli* bacteria.[23] In general, HC changes the water flow by creating turbulence and a pressure drop when installed in a water pipe. HC is a promising additive-free method for disinfecting drinking water,[24] but studies on its effects on drinking water biofilms remain scarce.

An alternating electromagnetic field is another specific treatment that can generate nanobubbles in water. Rapidly changing magnetic fields can destabilize dissolved gas, leading to the formation of nanobubbles.[25] Magnetic water treatment (MWT) has been shown to affect mineral scaling in water systems.[26] The mechanism is partly unclear and has been explained, for example, by OH^- radicals created by collapsing nanobubbles, as well as the dissolution of $CaCO_3$ resulting from nanobubble-nanoparticle clustering.[25,27] MWT can also affect biofilms, possibly due to the formation of nanobubbles and changes in pipe morphology and surface deposits, although such studies with drinking water biofilms are rare. In a study using natural river water, electromagnetic field treatment promoted the growth of planktonic microorganisms but limited the growth of microorganisms in the biofilm on stainless steel, also having a qualitative effect on the populations.[28] In another study using a pilot drinking water network, MWT had a varying impact on microbial growth and communities, depending on the pipe material.[29] The mechanism of action can be transmitted through nanobubbles generated in the process. The impact of MWT likely depends on the frequencies used, the pipe materials, and other factors.

This journal is © The Royal Society of Chemistry 2026

Environ. Sci.: Water Res. Technol., 2026, **12**, 1264–1279 | 1265

The pipe material has also been shown to affect the biofilm quantity and microbial communities.[29–31] However, there is still no consensus on which materials support the strongest growth and *vice versa*.[32] Moreover, biofilm studies on drinking water distribution systems often focus on qualitative analyses, such as determining microbial community structures, which may be partly due to the difficulty of quantitative sampling. However, quantitative analysis is essential when examining the mitigation of biofilm growth.[10]

This study investigated the effects of hydrodynamic cavitation and magnetic water treatment combined with different plumbing materials on biofilms in a pilot drinking water network. The aim was to evaluate the performance of commercially available HC and MWT devices under realistic distribution-system conditions. Biofilms were sampled quantitatively using a new biofilm-removal tool and analyzed both quantitatively and qualitatively at various time points during the biofilm lifecycle.

Experimental

Configuration of the pilot system

The pilot-scale water distribution network consisted of eight parallel loops of pipe mounted on the laboratory wall, of which seven loops were included in this study. Each pipe loop consisted of a 3.67 m-long water pipe with five pipe collectors (detachable pieces of pipe), which were approximately 30 cm long and had inner diameters of 1.4 cm (steel) and 1.6 cm (copper and PEX). Each collector had a separate shut-off valve at both ends, allowing for the collection of a water sample after the collector was detached from the system. The loops consisted of two copper, two stainless steel, and three PEX pipes (purchased from Onninen Ltd, Finland). The pipes were new and had not been used before the experiment. One line of each material was equipped with a 10 cm-long SIO nanobubble generator (SIO USA, USA; purchased from EOD Ltd, Finland), applying HC forces to the water flowing through. In addition, one PEX line was equipped with an MWT device (Bauer Solutions, Finland). The lines without devices worked as control lines. Fig. 1 shows the configuration of the pilot network, and Fig. 2 shows the appearance of the HC and MWT devices.

The water flow in the pilot system was set to simulate the water usage of an office building, primarily used during weekdays. Each line was flushed for 5 minutes, followed by a one-minute break before flushing the next line. There were four such flushing cycles per day from Monday to Friday. The water was supplied to the system *via* a pressure-regulated pump. A small, open-top buffer tank was used on the pump inlet to maintain constant pressure and provide decoupling from the building's water system. The drinking water for the experiment was supplied by a municipal waterworks plant, using surface water as the source. The raw water was treated with sedimentation, flotation, filtration, and disinfection with sodium hypochlorite.[33]

Sampling and quantitative analyses

The pilot system was put into operation in February 2023. The experiment lasted 16 months, with sampling conducted approximately every three months, except for the first
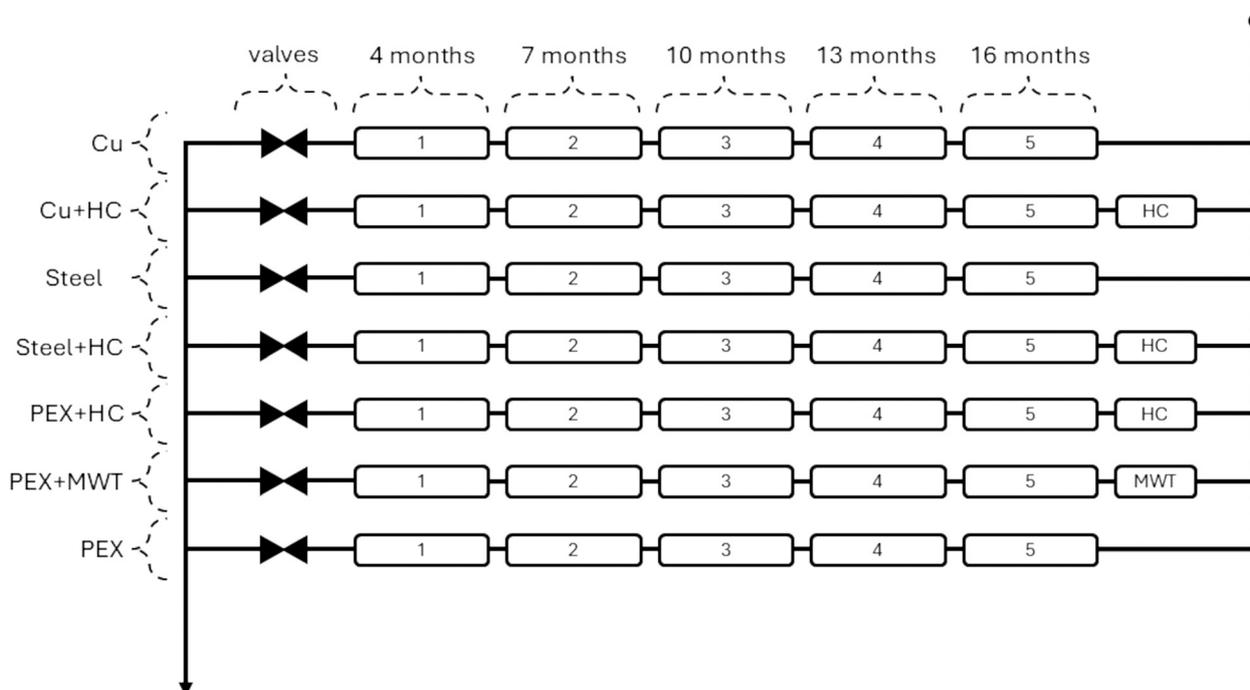

Fig. 1 Configuration of the pilot drinking water network used in this study.

Fig. 2 SIO nanobubble generator and Bauer MWT device installed into two pipelines of the pilot network.

samples, which were collected four months after the start. Every sampling started by removing one pipe collector from each parallel pipeline and pouring the water into a sterile tube. Biofilm was scraped from every pipe collector into a 50 ml sterile conical tube containing 15 ml Ringer's solution (8.5 g NaCl per L, 0.044 g Na_2HPO_4 per L, 0.023 g NaH_2PO_4 per L) using an aseptic biofilm-removal tool. After scraping the biofilm into the tube, the tool head was lightly shaken in the buffer solution to remove biofilm adhering to it.

The biofilm samples were homogenized in Ringer's solution by sonicating in a water bath using the Elmasonic S 70 H (Elma Schmidbauer GmbH, Germany) for 1 or 3 min, followed by vortexing.

Quantitative analysis of the biofilm samples was performed using the ATP and plate count methods. The ATP levels of each homogenized sample were measured using the ATP biomass kit (Biothema, Sweden), with three parallel samples measured in each case. The ATP amounts (pg) in the samples were calculated according to the manufacturer's instructions.

Additionally, aliquots of homogenized samples (and their dilutions) were grown on R2A (Merck, Germany) plates for up to 13 days at 22 °C. A 7-day incubation time was found to be insufficient for sonicated samples (data not shown).

Statistical analysis for quantitative ATP results was conducted in Jamovi (version 2.7), applying linear regression and factorial ANOVA to evaluate the effects of material, time, and treatment on biofilm levels.[34–37]

Pipe biofilm-removal tool

The biofilm-removal tool was designed for this study and fabricated using 3D printing, as shown in Fig. 3. The functional part of the biofilm removal tool consisted of three components: 1) an elastic double piston, 2) plastic washers, and 3) tightening nuts. The tool's pull rod was fabricated from a 3 mm stainless steel threaded rod to facilitate the

installation of other components. In addition to these parts, a plastic handle was fabricated for pulling the tool through the pipe, and an auxiliary tool was designed for installing and tightening the clamping nut. The special double piston was partially hollowed and printed in elastomer (Recreus, Filaflex 82A). The washers at both ends of the piston were printed in PETG. The two lips of the piston keep the piston in a perpendicular position when the tool is pulled through the pipe. Additionally, the piston diameter can be slightly adjusted using the tightening nut. A separate set of disposable washers and pistons was manufactured for each pipe size.

The tool's performance was tested by using three 25 cm-long pipe samples cut from the same PEX pipe (diameter 1 cm) containing a several-year-old biofilm. The biofilm was removed from each pipe sample into a 50 ml sterile conical tube containing 15 ml Ringer's solution using an aseptic biofilm-removal tool. To assess removal efficiency, the procedure was repeated twice in a new buffer tube, using a new tool head each time.

All biofilm samples were homogenized in Ringer's solution by sonicating in a water bath using the Elmasonic S 70 H for 3 min, followed by vortexing. Quantitative analysis of the samples was performed utilizing the ATP method, with three parallel samples measured in each case.

DNA extraction, amplification of bacterial ribosomal RNA, and DNA sequencing

Sample preparation and sequencing were performed at the Biocenter Oulu Sequencing Center (Oulu, Finland). Genomic DNA was extracted using the DNeasy PowerSoil Pro kit (Qiagen, Hilden, Germany) according to the manufacturer's protocol, with the exception that microbial material from suspended biofilm preparations was collected immediately after thawing by centrifugation (5000× g for 10 min). The supernatant was carefully removed, and pelleted microbes were resuspended in 750 µl of CD1 buffer.

The 16S ribosomal RNA gene (16S rRNA) was amplified from DNA by polymerase chain reaction (PCR) using slightly
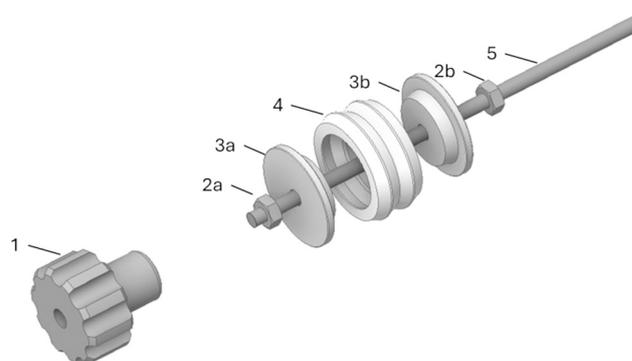

Fig. 3 Construction of the biofilm-removal tool (1 nut tightening tool, 2a + b nut, 3a + b plastic washer, 4 double piston, and 5 threaded rod).

This journal is © The Royal Society of Chemistry 2026

Environ. Sci.: Water Res. Technol., 2026, **12**, 1264–1279 | **1267**

modified 27F (5′-GACCAGGGTACGGTGRGTTYGATYMTGGC TCAG-3′) and 1492R (5′-CAGAGAGGCTCCGTGRGYTACCTT GTTACGACTT-3′) primers.[38] The PCR reactions were performed in 2 × 15 μl volumes, each containing 1× Phusion flash high-fidelity master mix (ThermoFisher Scientific, Waltham, MA, USA), 0.5 μM primers, and template DNA. After an initial 3-minute denaturation at 98 °C, the following conditions were used: 98 °C for 10 seconds, 52 °C for 30 seconds, 72 °C for 60 seconds. The final extension step was performed at 72 °C for 5 minutes. The number of amplification cycles was either 32 or 40, depending on the amount of microbial DNA in the specific sample.

After amplification, duplicate reactions were pooled together, and the amplification products were purified using the Ampure XP PCR purification reagent (Beckman Coulter, Brea, CA, USA). The concentration of amplicons was measured with a Quant-IT PicoGreen dsDNA assay kit (ThermoFisher Scientific). Samples with higher DNA concentrations were diluted to a range of 0.5–3 ng μL^{-1} before the indexing reaction.

Sample indexing was performed by PCR using primers that contained a second tail sequence, a 12-nt unique index sequence, and the first tail sequence. As a result, all samples contained a unique 12-nt index combination at the end of reads. The indexing PCR reactions were performed in 25 μl volumes, each containing 1× Phusion flash high-fidelity master mix, 0.5 μM indexing primer mix, and less than 5 ng of template DNA. After an initial 3-minute denaturation at 98 °C, the following conditions were used for 8 cycles: 98 °C for 10 seconds, 56 °C for 30 seconds, and 72 °C for 60 seconds. The final extension step was performed at 72 °C for 5 minutes.

After indexing, the samples were repurified using the Ampure XP, and the final concentration was determined using a Picogreen reagent. Equimolar amounts of each sample were pooled together, and a pooled sample was further purified and size-selected using the Ampure XP reagent. Before sequencing, the final concentration was determined using the Picogreen reagent.

Sequencing library preparation was performed using the SQK-LSK114 ligation sequencing kit V14 (Oxford Nanopore, Oxford, UK) according to the manufacturer's protocol, with 200 fmol of pooled DNA. 25 fmol of the ligated library was loaded into a MIN-FLO114 (Oxford Nanopore) flow-cell and sequenced 72 hours with the Oxford Nanopore Mk1c instrument.

Bioinformatic analysis of sequencing reads

After sequencing, the raw data in POD5 files were basecalled into FASTQ format using the Dorado basecaller (version 0.8.0; https://github.com/nanoporetech/dorado) with the super accuracy (SUP) model and a minimum quality score filter of 18. Sequencing accuracy was assessed using the NanoporeQC R package (https://www.github.com/msuokas-bco/nanoporeQC). This package aligns a 3.6 kbp DNA control standard (CS) fragment to its known sequence and generates a histogram and summary statistics of sequencing accuracy.

Sample-specific sequence reads were demultiplexed and trimmed using the bco_demux_tool (https://www.github.com/msuokas-bco/bco_demux_tool). The vsearch_dereplicate.py script (https://www.github.com/msuokas-bco/support_scripts/) was used to generate a globally dereplicated sequence set. The script operates in a manner comparable to the VSEARCH plugin used in QIIME2.[39,40]

Taxonomic classification of the dereplicated reads was performed by aligning sequences using Minimap2[41,42] with the SILVA SSU NR reference database (version 138.2). Before alignment, the associated taxonomy file was processed with the taxreftool (https://www.github.com/msuokas-bco/taxreftool) to remove taxonomic ambiguities using keyword filtering and the dada2 matchgenera function.[43]

Alignments were conducted against all archaeal and bacterial SSU sequences, along with 20 000 randomly selected eukaryotic SSU sequences, using Minimap2's high-accuracy long-read settings (k-mer size = 19, minimizer window = 5). The resulting alignment file was processed with the alignment_to_taxa.py script (https://msuokas-bco/support_scripts/), which converts data into taxonomically classified features. Unique alignments were assigned as direct reference matches, while sequences with multiple alignments were assigned using the lowest common ancestor (LCA) technique, provided the alignment scores were within a 97% threshold of each other. The abundance table was updated accordingly to reflect the abundance of merged features.

The data analysis steps were carried out in R version 4.4.2 using several bioconductor project packages. Data was first imported into the TreeSummarizedExperiment (TSE) object using the mia R package. Relative composition, alpha and beta diversity, and differential abundance of taxa in the samples were analysed using the following Bioconductor project packages: mia,[44] miaViz,[45] scater,[46] and vegan.[47]

Results and discussion

Biofilm removal and homogenization

The biofilms in the pipe collectors were removed as quantitatively as possible for analysis. Mechanical scraping, combined with sonication, is an effective method for collecting biofilms from plates or disks.[48] However, quantitative removal is not that straightforward from the inner surfaces of pipes. Previously, only a few methods have been reported, such as shaking the pipe collectors with glass beads and brushing with sterile brushes, for which quantitative effectiveness has not been demonstrated.[19,29]

In this study, a new pipe biofilm-removal tool utilizing 3D printing technology was developed for the mechanical removal of biofilms from the inner surfaces of pipe collectors. Fig. 3 illustrates the construction of the pipe biofilm-removal tool, and Fig. 4 demonstrates its effectiveness, showing the appearance of the pipe walls
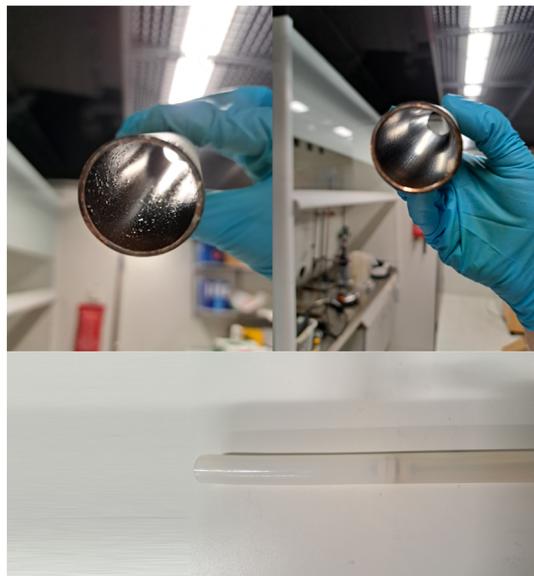
Fig. 4 Above, an older copper tube before (left) and after (right) biofilm removal. Below, a biofilm-removal tool inside a PEX pipe. The tool is moving towards the browner end of the pipe. The lighter end of the pipe is already scraped clean.

before and after treatment. The tool's advantages include adaptability to various pipe sizes, ease of use, and quick use,

as well as the even removal of biofilm from the entire inner pipe area.

The performance of the biofilm-removal tool was evaluated using three parallel PEX pipe samples. Each pipe sample was scraped three times, using a new tool head each time. Biofilm living biomass was quantified using the ATP method. The second scraping of the pipe yielded approximately 1.2% of the ATP obtained after the first scraping. The third scraping of the pipe yielded approximately 0.4% of the ATP obtained after the first scraping. Thus, as much as 98% of the biofilm could be removed by scraping the pipe once, supporting the quantitative nature of the tool. The recovery percentage may decrease when the biofilm mass in the pipe is low.

After being collected into a conical tube containing buffer solution, the biofilm samples were sonicated for homogenization. Various sonication durations were evaluated to optimize homogenization without compromising cell viability. A 1-minute sonication was sufficient for young biofilms up to 7 months, whereas longer sonication was required for later samples. The quantitative data from the third time point (10 months) are not included in the results because of excessive variation between parallel ATP measurements (data not shown). At this point, the 1-minute sonication was no longer
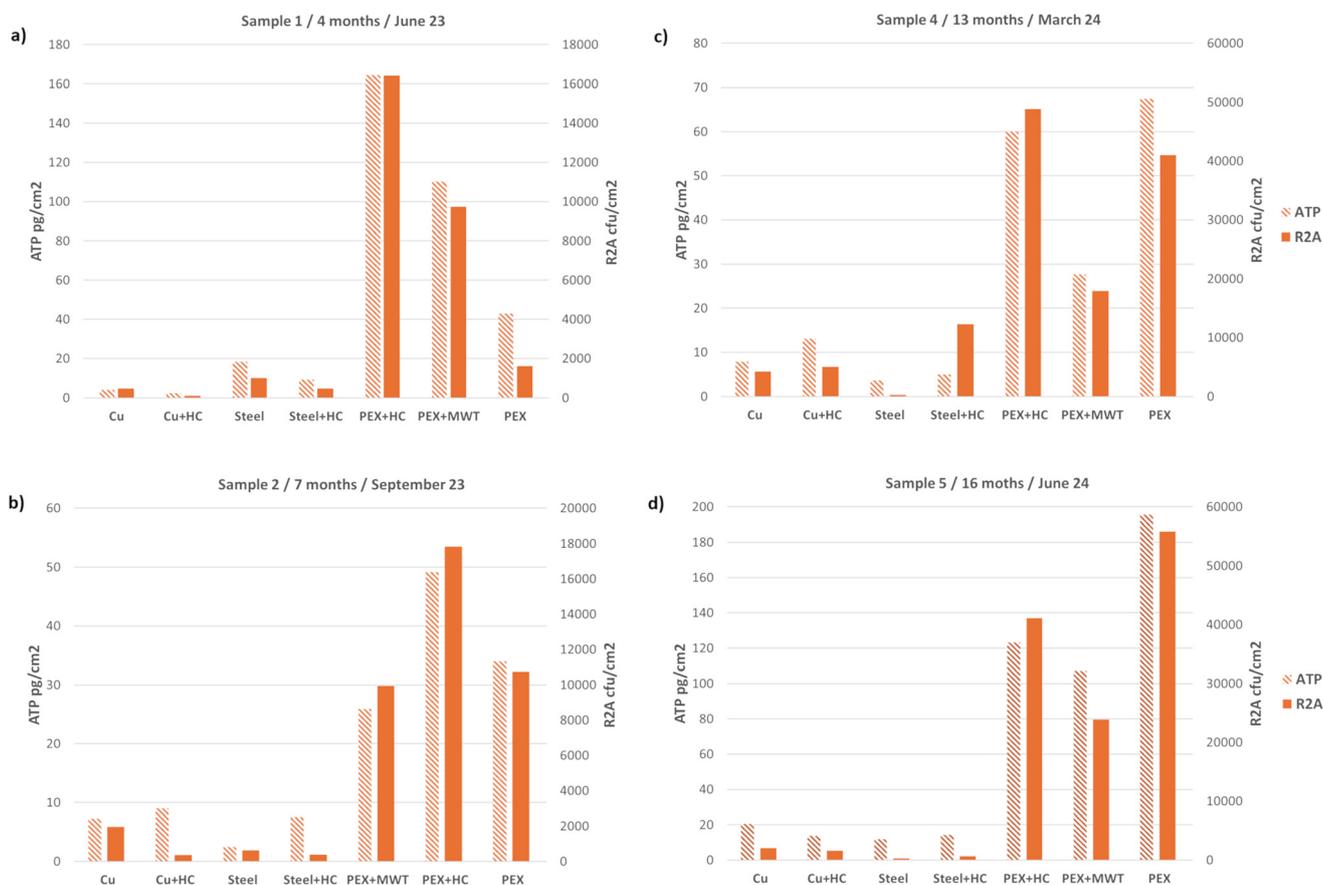

Fig. 5 ATP and R2A plate count values were calculated per pipe collector inner surface area at different sampling points, which were a) 4 months, b) 7 months, c) 13 months, and d) 16 months.

considered sufficient, as the biofilm structure had developed stronger over time. The accepted error between the parallel samples in ATP measurements was 10% or less. With 13- and 16-month samples, the sonication time was increased to 3 minutes.

Homogenized biofilm samples were quantitatively analyzed using ATP measurement and the R2A plate count

method. These methods have been successfully applied for biofilm quantification.[29,48,49]

Quantitative analyses

Effect of pipe material on biofilm growth. Fig. 5 shows the ATP values and R2A plate count calculated per pipe collector
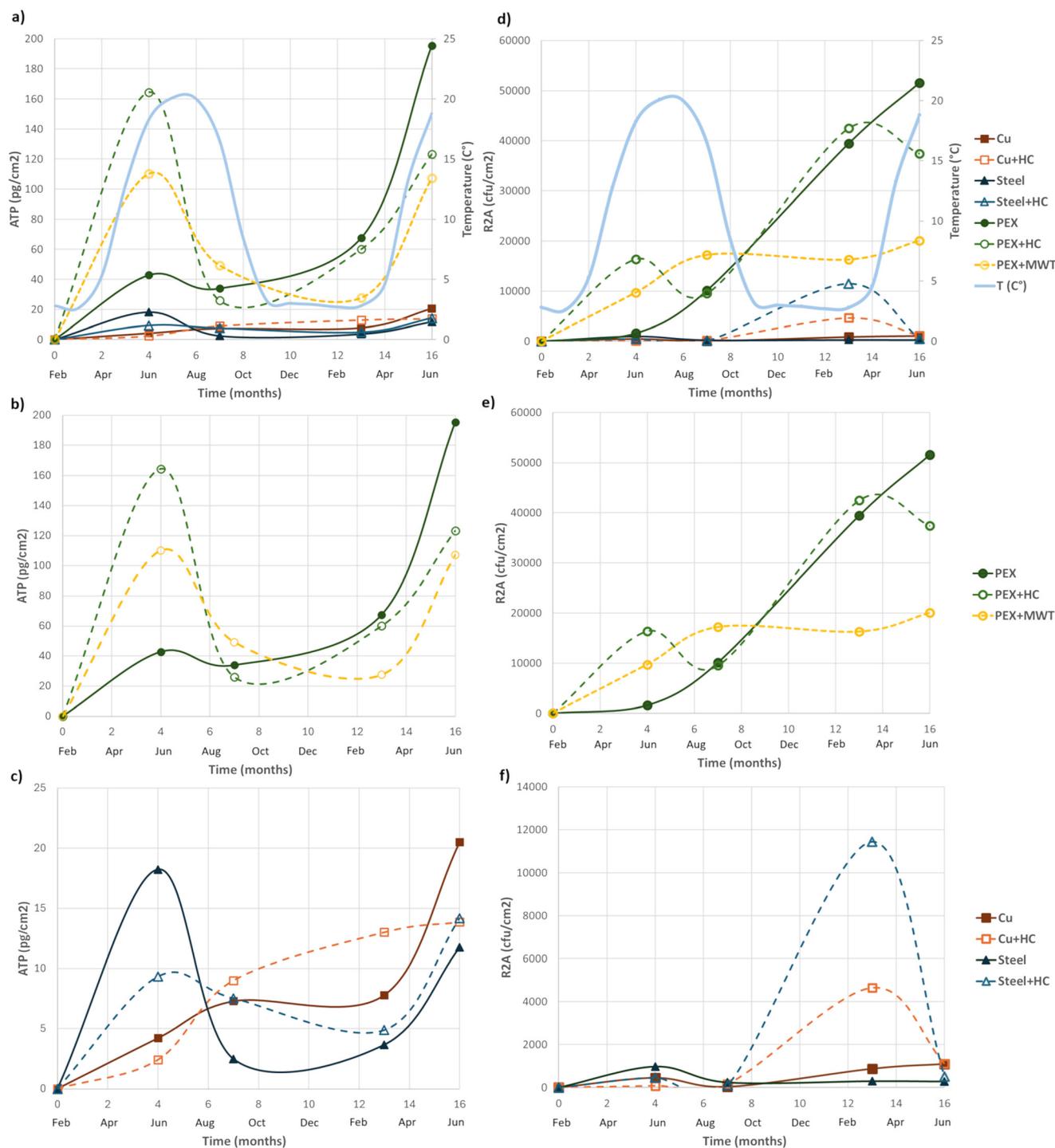
Fig. 6   a)–c) ATP and d)–f) R2A plate count values calculated per pipe collector inner surface area at different sampling time points. The water temperature (a and d) was measured from purified water at the waterworks.

1270 | Environ. Sci.: Water Res. Technol., 2026, 12, 1264–1279

This journal is © The Royal Society of Chemistry 2026

inner surface area at different sampling points, which were 4 (Fig. 5a), 7 (Fig. 5b), 13 (Fig. 5c), and 16 (Fig. 5d) months.

Fig. 6 shows the ATP values (Fig. 6a–c) and R2A plate count (Fig. 6d–f) calculated per pipe collector inner surface area at different sampling time points.

Pipe material, as well as other environmental conditions, are known to affect biofilm formation in drinking water networks. The surface roughness, which often increases over time due to material deterioration or corrosion, plays a crucial role in biofilm attachment. Also, organic additives used in the production of the pipes can leach from the material and act as nutrients for biofilm bacteria.[50]

This study investigated biofilm growth on copper, stainless steel, and PEX pipes. Copper is a traditional plumbing material known for its safety and durability. Metallic copper and copper alloys remain commonly used materials in plumbing systems. Stainless steel is an excellent, yet expensive, pipe material typically used in challenging positions that require extra durability. Following the plastic revolution, PEX became a popular plumbing material due to its low cost and corrosion-resistant nature. Due to slight variations in diameter, the water flow rate was approximately 1 m s^{-1} in PEX and copper pipes and 1.3 m s^{-1} in steel pipes, both typical premise plumbing flow rates. Although very high flow rates have been shown to offer some advantage in biofilm control, the flow rates used in this study do not reach such velocities.[51]

As shown in Fig. 5, the results indicate that the metallic materials used in this study support lower biofilm growth compared to PEX. In the 16-month timeline, steel pipes show very moderate biofilm growth. Possibly, the smooth surface of stainless steel hinders the attachment of biofilm. Moreover, steel pipes are not expected to release organic molecules or additives that could work as nutrients. Copper also showed better performance in mitigating biofilm when compared to PEX. Copper is recognized for its antimicrobial properties, which can inhibit biofilm formation in plumbing systems. However, the leaching of copper ions from the pipes will likely slow down after the formation of an oxidation layer, which typically takes up to 6 months. This may also affect biofilm formation and could be the reason for minimal growth in copper pipes at the first sampling point (Fig. 5a). Despite the antimicrobial characteristics of copper, the literature on its use to inhibit biofilm growth is somewhat controversial.[52] Learbuch et al. observed lower biofilm growth on copper compared to plastic materials.[53] However, Inkinen et al. detected lower microbial counts in PEX than copper pipes.[29]

This study suggests that during the 16-month research period, PEX supports significantly higher biofilm growth than stainless steel and copper. The statistical analysis also indicated that pipe material had a significant effect on ATP values ($p < 0.001$). The rapid onset of biofilm growth in the first sample (Fig. 5a) within the PEX pipes may be attributed to organic additives or degradation products leaching from the pipes, serving as nutrient sources for microbes, thereby enhancing biofilm growth. For example, the amounts of tert-butyl alcohol (TBA) and methyl tert-butyl ether (MTBE) released from new PEX-a pipes are known to be high in the first three months of use.[33]

Probably, due to the multiple variables changing among studies, there is no consensus on which type of pipe material is best or worst in terms of biofilm growth or mitigation. Both metallic and polymeric materials have been associated with biofilm development.[10,54] Some studies suggest that the effect of the pipe material on biofilm quantity and quality may decrease over the long term.[30,55] Many studies, especially those with quantitative analysis, have not been conducted in realistic conditions, which hinders the applicability of the results. Additionally, the quantitative removal of biofilm from the inner surfaces of pipes is challenging, which may lead to variations between studies.

Biofilm dynamics due to annual variations. Biofilm is a dynamic system; several environmental factors affect the number of live microbes and microbiota composition.[56] Seasonal variations are likely due to fluctuations in water temperature, chlorine levels, oxygen levels, and organic matter levels, as well as the presence of microbes in the water.

The results in Fig. 6 show significant variation in biofilm abundance across time points. Variations in biofilm amounts are highest with PEX pipes, likely due to greater accumulation within them. In the statistical analysis accounting for the effects of materials, time, and treatments, time had no significant effect on ATP levels, likely due to substantial variations that seem random across time.

Fig. 6 also shows the monthly variations of water temperature. Water temperature appears to correlate with ATP levels in biofilms (Fig. 6a), although the peaks do not align precisely. The temperature was measured at the waterworks; therefore, it may differ slightly from the temperature at the pilot network. Other variables measured at the waterworks, such as chlorine, oxygen, and organic matter, exhibited less variation throughout the year and did not show significant correlations with biofilm levels in the pilot network (data not shown). Notably, temperature changes have also been shown to affect nanobubbles whose characteristics are not yet fully understood. For example, nanobubble size and surface charge are temperature-dependent.[57,58] The results suggest that comparisons between different time points should be made with care. Instead, at a specific time point, comparison between various materials and treatments is easier.

Effect of HC and MWT on biofilm growth. Results shown in Fig. 5 and 6 suggest that HC and MWT enhance biofilm growth in PEX pipes during the initial stages of biofilm development. The mechanism may be related to increased oxygen or nutrient supply by nanobubbles.[59,60] The hydrophobic plastic surface attracts hydrophobic nanobubbles, which may enhance the release of VOC and antioxidants at the beginning of the study period.[33] This phenomenon is likely dependent on the specific

This journal is © The Royal Society of Chemistry 2026

Environ. Sci.: Water Res. Technol., 2026, **12**, 1264–1279 | 1271

characteristics of PEX quality. On the contrary, at the two final samplings (13 and 16 months), the effect of HC and MWT on biofilm growth seems opposite. Notably, MWT at later samplings appears to reduce biofilm growth in PEX pipes, as indicated by both ATP and R2A analysis. However, the statistical analysis showed no significant effect of the treatments on ATP levels.

The potential small effect of MWT on biofilm mitigation may be due to several different mechanisms. In addition to the mechanical effect of nanobubbles colliding with adherent material on the pipe surface, they are supposed to cause cell rupture in biofilms through ROS generation, pressure, and heat shocks caused by bubble collapse.[61] MWT is known to remove scales and prevent their formation.[26] Thus, biofilm mitigation may also be due to fewer scales that can work as a biofilm attachment and growth base. Unlike MWT, HC causes turbulence and pressure loss, which may explain differences in their effects.

With metallic materials, the effect of HC on ATP and plate count values is less pronounced, probably due to the overall lower amount of biofilm. Normal variations in the analyses may also cause some fluctuations. However, oxygen-containing nanobubbles may potentially increase the rate of copper oxidation and the release of Cu^{2+}.[62] This could speed up the formation of the protective oxidation layer on copper tubes.

In another study using the pilot drinking water network, MWT had varying effects on microbial growth, depending on pipe materials.[29] In ATP analysis, control copper pipes showed ATP counts higher than those with magnetic water treatment, and in PEX pipes, greater ATP values were found with magnetic water treatment than without it. The biofilms were 10–12 months old, and glass beads were used for biofilm removal, which may have made the analysis less quantitative. In qualitative analysis, biofilms from a copper pipe with magnetic water treatment exhibited higher species richness than those from the PEX pipeline with magnetic water treatment and from control copper and PEX pipes.[29]

As shown in Fig. 5, there is a correlation between the ATP and R2A values. However, ATP and R2A values cannot be compared straightforwardly. The ATP value should be directly proportional to the number of living bacterial cells in the sample (and possibly some newly dead cells of which ATP has not yet been degraded), although the presence of eukaryotic cells can cause some uncertainty.[63] In turn, the number of colonies on R2A plates represents only the microbes that can grow under the given conditions and does not encompass the entire microbiome in the samples. Thus, of these two methods, ATP measurement can be considered more reliable for biofilm quantification.[48] This is also supported by the more precise correlation between temperature and ATP than between temperature and plate count (Fig. 6).

Biofilm bacterial communities

Biofilms in water piping contain diverse microbial communities where different microbes interact synergistically. Like biofilm quantity, biofilm microbiota is also susceptible to various environmental factors and exhibits seasonal variations.[64]

Sequence analysis was included in this study to elucidate the development of biofilm communities during a 16-month study period on various pipe materials and under the influence of two different treatments (MWT, HC) or untreated water. The total number of demultiplexed and trimmed sequences in the data set was approximately 2.4 million, of which 2.3 million were unique. Of these, over 99.9% were successfully aligned to the Silva reference sequence set. Approximately 34% of sequences were aligned once, while the rest had multiple matches. After filtering SSU non-microbial data, the total number of microbial taxonomic features was 1337, and the total number of sequence counts was 1 926 086. Sample-specific count numbers ranged from 36 544 to 84 492.

Additionally, the accuracy of the nanopore sequencing run was studied by aligning sequences to a known DNA CS 3.6 kbp DNA sequence. Measured mean, median, and fifth percentile accuracies with 26 259 sampling depth were 99.46%, 99.61% and 98.44%, respectively. Results highlight a significant improvement in the accuracy of the latest sequencing chemistry and flow cells of the Oxford nanopore sequencing technology.

Community composition. Bar charts in Fig. 7 present the genus-level composition of biofilms in the samples. The most prevalent bacteria in all samples were *Gemmata*, *Hyphomicrobium*, *Pirellula*, *Sphingomonas*, *Novosphingobium*, *Planctopirus*, *Legionella*, *Methylobacterium*, and *Tabrizicola*. In copper samples, *Sphingomonas*, *Planctopirus*, and *Novosphingobium* were the dominant species. In steel samples, the same genera frequently dominated. In PEX samples, *Gemmata*, a member of the *Planctomycetes*, emerged as one of the top three genera, along with *Sphingomonas* and *Novosphingobium*. All these genera are typical in drinking water biofilms.[65] *Gemmata* has been previously identified on PEX pipes too.[29]

Across all materials, the community composition evolved over time. On copper, the early biofilms (4 and 7 months) were almost entirely *Sphingomonas and Planctopirus*. In later samples, there was a modest rise in *Novosphingobium*, but overall, the composition on copper surfaces remained relatively stable. On steel, *Sphingomonas* dominated throughout, with *Planctopirus* and *Novosphingobium* oscillating slightly over time. On PEX surfaces, *Sphingomonas* and *Pirellula* dominated in early samples (4 and 7 months). Later stages (13 and 16 months), on the other hand, showed an increased presence of *Gemmata and Novosphingobium*.

The heatmap presented in Fig. 8 shows the 25 most common bacterial features typically identified at the genus level. Clustering of samples falls well along pipe material,
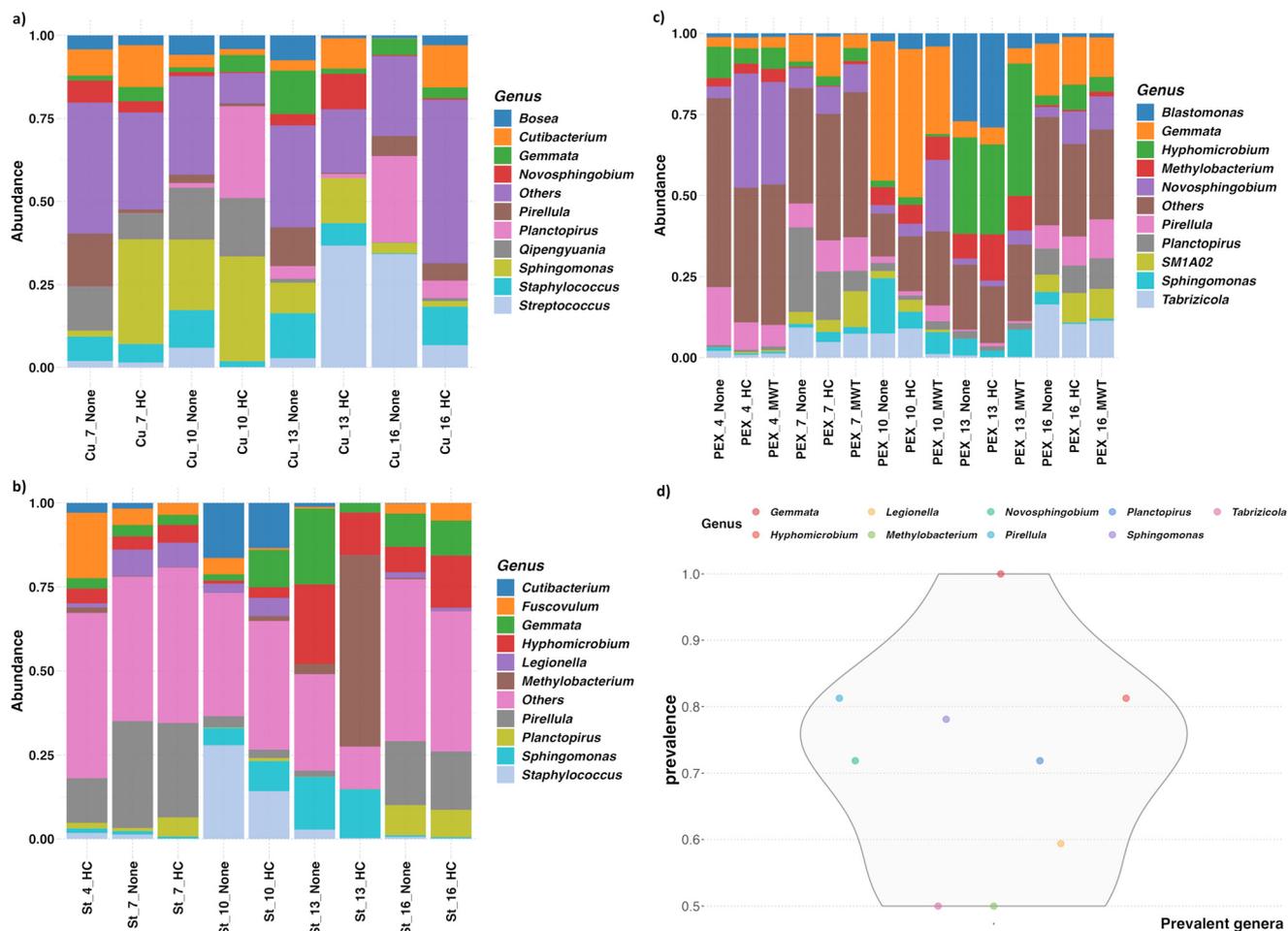
1272 | *Environ. Sci.: Water Res. Technol.*, 2026, **12**, 1264–1279

This journal is © The Royal Society of Chemistry 2026

Fig. 7 Genus-level biofilm composition for a) copper, b) steel, and c) PEX samples, grouped by treatment (HC, MWT, none), and d) the most prevalent genera in all samples.

meaning each material harbored a distinct subset of the top 25 genera. It is evident that different pipe surface materials favor different microbial communities. PEX may promote the growth of specific genera, while copper may suppress some of these or enrich others. In Fig. 8, no visible clustering by treatment is observed. Subtle shifts may exist (*e.g.*, a few *Gemmata* hotspots under MWT), but overall, the heatmap indicates that abundances fluctuate from sample to sample, rather than from treatment to treatment.

Legionella was detected in nearly all samples, but was more prominent in PEX samples than in copper or steel. It was present most in later PEX samples without treatment (1–2% relative abundance). The other classic opportunistic genera, *Mycobacterium* and *Methylobacterium*, were consistently present across all materials and sampling times (1–5% relative abundance), with *Mycobacterium* showing a modest increase in later PEX samples. Skin-associated genera, such as *Cutibacterium*, *Staphylococcus*, and *Streptococcus*, were detected on all materials but were more prominent on copper and steel, particularly in samples where assay results indicated low biomass levels. Thus, their presence might be the result of low-level contamination

during the assembly of the pilot network or sampling. Analyzing the communities with or without these taxa did not change the observed differences between the material or time-point groups (data not shown).

Alpha diversity. Alpha diversity, as described by the Shannon index, provides information on species richness and evenness within samples. In this study, alpha diversities ranged from 1.7 to 4.3, which is a typical level for premise plumbing biofilms in chlorinated water.[52,66] Species richness, *i.e.*, the number of microbial features per sample, varied from 140 to 373.

Fig. 9 shows the Shannon index for copper, steel, and PEX. Metal pipes hosted a relatively constrained, low-evenness biofilm that did not diversify over time, resulting in relatively few bacterial features dominating in biofilms. In contrast, PEX biofilms became more even over time, suggesting that the polymer surface could allow a broader array of taxa to establish as the biofilm matures. With PEX, it seems that during the summer months, except for the first sampling point, the biofilm may have been richer and more even than during other months of the year. The 13-month sample (March) with steel and PEX appears divergent, with
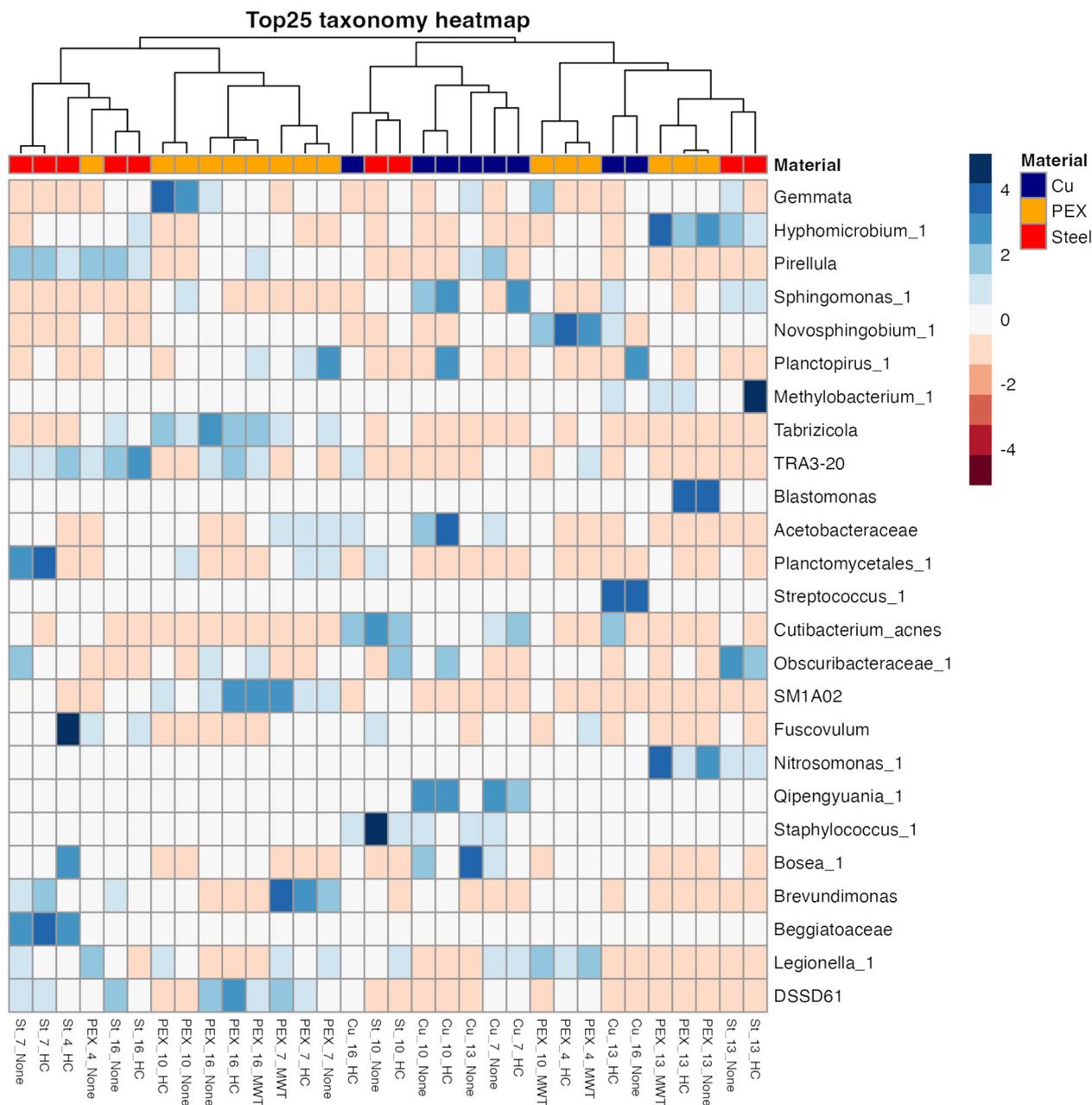
This journal is © The Royal Society of Chemistry 2026

Environ. Sci.: Water Res. Technol., 2026, **12**, 1264–1279 | **1273**

Fig. 8 The heatmap presentation of the sequencing results. Samples are clustered by correlation-based similarity to group similar biofilm communities.

lower Shannon values compared to other time points. However, statistical analysis revealed no significant differences in species richness among the different sample groups, except for biofilm age in PEX samples, which showed a statistically significant effect on diversity, as determined by the Kruskal–Wallis test. Treatment had a negligible impact on diversity across all material types at the sampling points.

The results suggest that biofilms in PEX pipes were inherently more dynamic, as also evidenced by the quantitative data. The absence of antimicrobial properties and potential nutrient leaching could lead to increased biofilm growth and more pronounced seasonal variations.

This finding is consistent with a previous study suggesting that biofilms on plastic pipes are more influenced by seasonal dynamics than those on other types of pipes.[56]

Beta diversity. Beta diversity, as measured by the Bray–Curtis dissimilarity index, reveals the differences in microbial community composition between samples. Fig. 10 shows the PCoA plots (multidimensionally scaled Bray–Curtis) for biofilm samples on copper, PEX, and steel pipes. Samples seem to cluster both by pipe material (Fig. 10a) and sample collection points (Fig. 10b). Microbial communities on PEX and copper were the most divergent, with steel samples lying in between.
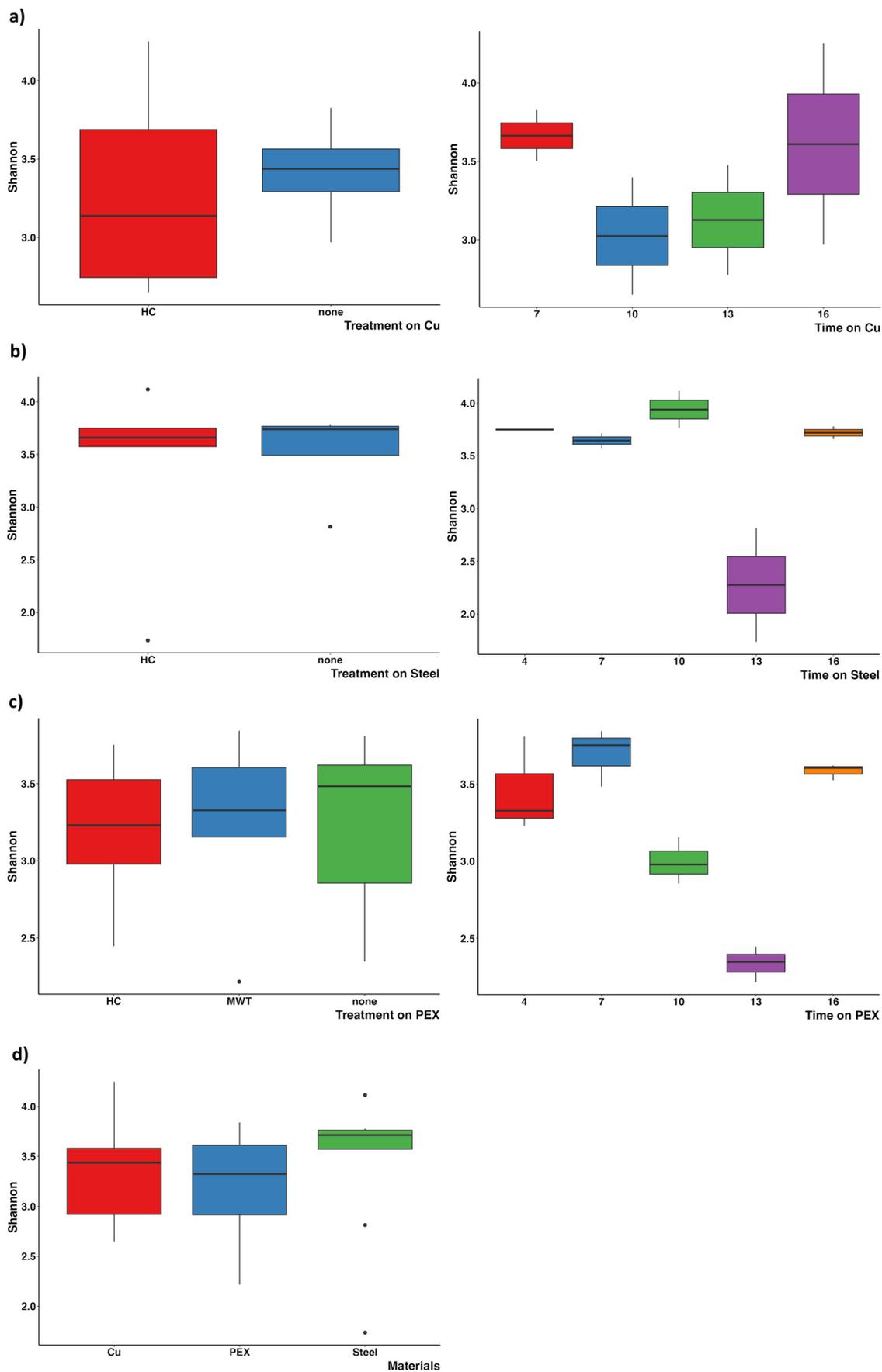
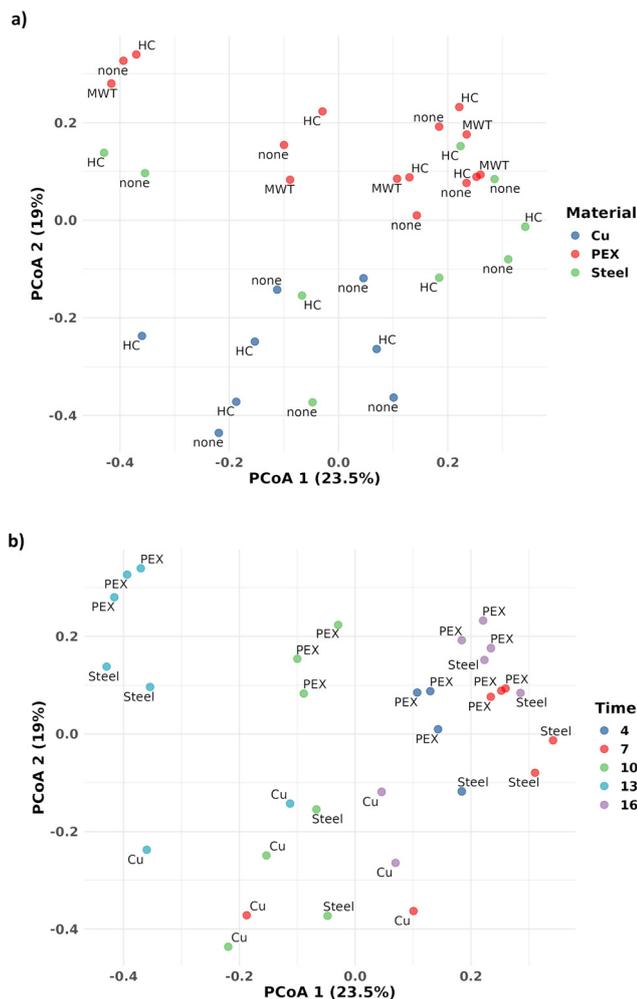Fig. 9   Shannon indices for a) copper, b) steel, and c) PEX samples, and d) between materials.

This journal is © The Royal Society of Chemistry 2026

Environ. Sci.: Water Res. Technol., 2026, **12**, 1264–1279 | **1275**

Fig. 10 Beta-diversity PCoA plots grouped by a) material and b) sampling time.

The pipe material creates a specific habitat for microbes, which is affected, for example, by surface roughness, influencing the trapping of particles and hydrodynamics in the vicinity of the surface. Moreover, surface chemistry determines the hydrophobicity or hydrophilicity of the surface, as well as the dissolution of ions or VOCs and precipitation of other compounds on the surface, and the reactions that occur in the vicinity of the surface.

Changes between different sample collection points likely reflect the dynamic nature of biofilm formation mentioned earlier, which contributes to the overall dispersion of samples belonging to the different pipe material groups. According to PERMANOVA analysis, time explains the largest share of variance (time $R^2 = 0.40$, $p < 0.001$; material $R^2 = 0.19$, $p < 0.001$). The water treatments in this study did not appear to have a significant effect on microbial communities, which may be partly due to the limited number of samples.

The 13-month time point stands out, with communities on steel and PEX differing significantly from those at other time points, as previously observed for alpha diversity. The 13-month sample was collected in March, when meltwater

typically affects the quality of raw water at waterworks. This may have caused the visible shift in microbial communities. Copper pipes do not exhibit this shift, possibly due to the antimicrobial properties of copper, which create a selective pressure on the biofilm community.

Conclusions

In this study, biofilm development and growth were investigated in a pilot drinking water network with different pipe materials and under the influence of magnetic water treatment and hydrodynamic cavitation during a 16-month study period. A quantitative pipe biofilm-removal tool was developed for collecting biofilm from pipe samples.

The results suggest that pipe material significantly affects biofilm levels. PEX supported higher biofilm growth than copper and steel. Among the metallic materials, stainless steel was slightly more effective than copper in mitigating biofilms. The seasonal variations in biofilm quantity were substantial in PEX pipes, correlating with water temperature. The impacts of MWT and HC on biofilm growth varied with time and material. In PEX pipes, they appeared to enhance biofilm growth during the early stages of biofilm development; however, with mature biofilms, they slightly inhibited growth, particularly MWT. With metallic materials, the effects were minor. The statistical analysis showed significant effects only for material, and more samples would be needed to confirm the effects of treatments. The microbial communities were most strongly affected by the pipe material and sampling time.

The potential impact of MWT and HC on biofilm growth within PEX pipes may be transmitted through nanobubbles, but other mechanisms are also possible. Future research should focus on detecting nanobubbles generated by MWT and HC devices and quantifying their presence in the current system. Analyzing nanobubbles is challenging, particularly in tap water containing various nanoscale impurities that are difficult to distinguish from nanobubbles.[67]

Nanobubbles have been studied for numerous applications, of which biofilm mitigation is only a small branch. Due to the many variables across studies and multiple mechanisms of action, the effects of nanobubbles can appear case-dependent. Further research on nanobubbles and their effects on biofilms is still required. Also, the longer-term impacts of pipe materials, MWT, and HC on biofilms should be clarified. The mild effect of HC on biofilm levels in this study indicates that alternative, more effective methods for introducing hydrodynamic cavitation for biofilm control need investigation. The sampling tool developed for this study facilitates future research by enabling the collection of quantitative samples from pipes.

Author contributions

Noora Salonen: writing – original draft, writing – review and editing, methodology, investigation, data curation; Kalle

1276 | *Environ. Sci.: Water Res. Technol.*, 2026, **12**, 1264–1279

This journal is © The Royal Society of Chemistry 2026

Conflicts of interest

There are no conflicts to declare.

Data availability

The raw sequences were submitted to GenBank under the bioproject accession number PRJNA1285824. Other data will be made available on request.

Acknowledgements

References

1 X. Chen, L. Xiao, J. Niu, Y. Wang, X. Zhang and L. Gong, et al., Early succession of biofilm bacterial communities in newly built drinking water pipelines via multi-area analysis, Appl. Microbiol. Biotechnol., 2023, 107, 3827–3828.

2 N. Salonen, M. Ahonen, K. Sirén, R. Mäkinen, V.-J. Anttila and M. Kivisaari, et al., Methods for infection prevention in the built environment — a mini-review, Front. Built Environ., 2023, 9, 1212920.

3 D. L. Zubris, K. P. C. Minbiole and W. M. Wuest, Polymeric quaternary ammonium compounds: versatile antimicrobial materials, Curr. Top. Med. Chem., 2017, 17, 305–318.

4 I. M. Oliveira, I. B. Gomes, L. C. Simões and M. Simões, A review of research advances on disinfection strategies for biofilm control in drinking water distribution systems, Water Res., 2024, 253, 121273.

5 F. García-Ávila, L. F. del Pino, G. Bonifaz-Barba, C. Zhindón-Arévalo, L. Ramos-Fernández and D. García-Altamirano, et al., Effect of residual chlorine on copper pipes in drinking water systems, J. Eng. Sci. Technol. Rev., 2019, 12, 119–126.

6 D. Hanigan, L. Truong, M. Simonich, R. Tanguay and P. Westerhoff, Zebrafish embryo toxicity of 15 chlorinated, bromated, and iodinated disinfection by-products, J. Environ. Sci., 2017, 58, 302–310.

7 T. Sasada, T. Hinoi, Y. Saito, T. Adachi, Y. Takakura and Y. Kawaguchi, et al., Chlorinated water modulates the development of colorectal tumors with chromosomal instability and gut microbiota in Apc-deficient mice, PLoS One, 2015, 10, e0132435.

8 D. Martino, The effects of chlorinated drinking water on the assembly of the intestinal microbiome, Challenges, 2019, 10, 10.

9 S. Khan, T. K. Beattie and C. W. Knapp, Rapid selection of antimicrobial-resistant bacteria in complex water systems by chlorine and pipe materials, Environ. Chem. Lett., 2019, 17, 1367–1373.

10 P. Erdei-Tombor, G. Kiskó and A. Taczman-Brückner, Biofilm formation in water distribution systems, Processes, 2024, 12, 280.

11 E. P. Favvas, G. Z. Kyzas, E. K. Efthimiadou and A. C. Mitropoulos, Bulk nanobubbles, generation methods and potential applications, Curr. Opin. Colloid Interface Sci., 2021, 54, 101455.

12 T. Vehmas and L. Makkonen, Metastable nanobubbles, ACS Omega, 2021, 6, 8021–8027.

13 A. J. Atkinson, O. G. Apul, O. Schneider, S. Garcia-Segura and P. Westerhoff, Nanobubble technologies offer opportunities to improve water treatment, Acc. Chem. Res., 2019, 52, 1196–1205.

14 K. R. Marcelino, L. Ling, S. Wongkiew, H. T. Nhan, K. C. Surendra and T. Shitanaka, et al., Nanobubble technology applications in environmental and agricultural systems: Opportunities and challenges, Crit. Rev. Environ. Sci. Technol., 2023, 53, 1378–1403.

15 S. Haris, X. Qiu, H. Klammler and M. M. A. Mohamed, The use of micro-nano bubbles in groundwater remediation: A comprehensive review, Groundw. Sustain. Dev., 2020, 11, 100463.

16 K. Ebina, K. Shi, M. Hirao, J. Hashimoto, Y. Kawato and S. Kaneshiro, et al., Oxygen and air nanobubble water solution promote the growth of plants, fishes, and mice, PLoS One, 2013, 8, e65339.

17 Y. Wu, T. Lyu, B. Yue, E. Tonoli, E. A. M. Verderio and Y. Ma, et al., Enhancement of tomato plant growth and productivity by agri-nanotechnology using nanobubble oxygation, J. Agric. Food Chem., 2019, 67, 10823–10831.

18 S. Shiroodi, M. H. Schwarz, N. Nitin and R. Ovissipour, Efficacy of nanobubbles alone or in combination with neutral electrolyzed water in removing Escherichia coli O157:H7, Vibrio parahaemolyticus, and Listeria innocua Biofilms, Food Bioprocess Technol., 2021, 14, 287–297.

19 Y. Xiao, S. C. Jiang, X. Wang, T. Muhammad, P. Song and B. Zhou, et al., Mitigation of biofouling in agricultural water distribution systems with nanobubbles, Environ. Int., 2020, 141, 105787.

20 A. Luo, T. Wang, P. Luo, Z. Zheng, M. Fiallos and Y. Bian, et al., Mechanism by which micro-nano bubbles impact biofilm growth in drinking water distribution systems, Environ. Sci.: Water Res. Technol., 2025, 11, 754–767.

21 P. Unger, A. S. Sekhon, S. Sharma, A. Lampien and M. Michael, Impact of gas ultrafine bubbles on the efficacy of antimicrobials for eliminating fresh and aged Listeria monocytogenes biofilms on dairy processing surfaces, J. Food Saf., 2023, e13057.

This journal is © The Royal Society of Chemistry 2026

Environ. Sci.: Water Res. Technol., 2026, 12, 1264–1279 | 1277

22 P. Khan, W. Zhu, F. Huang and W. Gao, Rapid selection of antimicrobial-resistant bacteria in complex water systems by chlorine and pipe materials, *Water Supply*, 2020, **20**, 2021–2035.

23 S. Han, S. Lee and Y. S. Joung, Long-term effect of nanobubbles generated by turbulent flow through diamond-pattern notches on liquid properties, *Results Eng.*, 2022, **14**, 100375.

24 X. Sun, J. Liu, L. Ji, G. Wang, S. Zhao, J. Y. Yoon and S. Chen, A review on hydrodynamic cavitation disinfection: the current state of knowledge, *Sci. Total Environ.*, 2020, **737**, 139606.

25 N. V.-Y. Quach, A. Li and J. C. Earthman, Interaction of calcium carbonate with nanobubbles produced in an alternating magnetic field, *ACS Appl. Mater. Interfaces*, 2020, **12**, 43714–43719.

26 M. Latva, J. Inkinen, J. Rämö, T. Kaunisto, R. Mäkinen and M. Ahonen, *et al.*, Studies on the magnetic water treatment in new pilot scale drinking water system and in old existing real-life water system, *J. Water Process Eng.*, 2016, **9**, 215–224.

27 A. Ghadimkhani, W. Zhang and T. Marhaba, Ceramic membrane defouling (cleaning) by air nano bubbles, *Chemosphere*, 2016, **146**, 379–384.

28 A. Mercier, J. Bertaux, J. Lesobre, K. Gravouil, J. Verdon and C. Imbert, *et al.*, Characterization of biofilm formation in natural water subjected to low-frequency electromagnetic fields, *Biofouling*, 2016, **32**, 287–299.

29 J. Inkinen, B. Jayaprakash, M. Ahonen, T. Pitkänen, R. Mäkinen and A. Pursiainen, *et al.*, Bacterial community changes in copper and PEX drinking water pipeline biofilms under extra disinfection and magnetic water treatment, *J. Appl. Microbiol.*, 2018, **124**, 611–624.

30 M. J. Lehtola, I. T. Miettinen, M. M. Keinänen, T. K. Kekki, O. Laine and A. Hirvonen, *et al.*, Microbiology, chemistry and biofilm development in a pilot drinking water distribution system with copper and plastic pipes, *Water Res.*, 2004, **38**, 3769–3779.

31 W. Tang, Q. Li, L. Chen, W. Zhang and H. Wang, Biofilm community structures and opportunistic pathogen gene markers in drinking water mains and the role of pipe materials, *ACS ES&T Water*, 2021, **1**, 630–640.

32 A. C. Cullom, R. L. Martin, Y. Song, K. Williams, A. Williams and A. Pruden, *et al.*, Critical Review: Propensity of premise plumbing pipe materials to enhance or diminish growth of *Legionella* and other opportunistic pathogens, *Pathogens*, 2020, **9**, 957.

33 A. Pelto-Huikko, M. Ahonen, M. Ruismäki, T. Kaunisto and M. Latva, Migration of volatile organic compounds (VOCs) from PEX-a pipes into the drinking water during the first five years of use, *Materials*, 2021, **14**, 746.

34 The jamovi project, *jamovi* (Version 2.7) [computer software], 2025, Available from: https://www.jamovi.org.

35 R Core Team. *R: A language and environment for statistical computing* (Version 4.5) [computer software], 2025, Available from: https://cran.r-project.org (R packages retrieved from CRAN snapshot 2025-05-25).

36 J. Fox and S. Weisberg, *car: Companion to Applied Regression* [R package], 2024, Available from: https://cran.r-project.org/package=car.

37 R. Lenth, *emmeans: Estimated Marginal Means, aka Least-Squares Means* [R package], 2025, Available from: https://cran.r-project.org/package=emmeans.

38 D. J. Lane, *16S/23S rRNA sequencing. Nucleic acid techniques in bacterial systematics*, ed. E. Stackebrandt and M. Goodfellow, John Wiley & Sons, Chichester, 1991, pp. 115–175.

39 E. Bolyen, J. R. Rideout and M. R. Dillon, *et al.*, Reproducible, interactive, scalable and extensible microbiome data science using QIIME 2, *Nat. Biotechnol.*, 2019, **37**, 852–857.

40 T. Rognes, T. Flouri, B. Nichols, C. Quince and F. Mahé, VSEARCH: a versatile open source tool for metagenomics, *PeerJ*, 2016, **4**, e2584.

41 H. Li, Minimap2: pairwise alignment for nucleotide sequences, *Bioinformatics*, 2018, **34**, 3094–3100.

42 H. Li, New strategies to improve minimap2 alignment accuracy, *Bioinformatics*, 2021, **37**, 4572–4574.

43 B. J. Callahan, P. J. McMurdie, M. J. Rosen, A. W. Han, A. J. A. Johnson and S. P. Holmes, High-resolution sample inference from Illumina amplicon data, *Nat. Methods*, 2016, **13**, 581–583.

44 T. Borman, F. Ernst and S. Shetty, mia: Microbiome analysis, *R package version 1.13.47*, 2024.

45 T. Borman, F. Ernst and L. Lahti, miaViz: Microbiome Analysis Plotting and Visualization, *R package version 1.13.14*, 2024.

46 D. J. McCarthy, K. R. Campbell, A. T. L. Lun and Q. F. Willis, Scater: pre-processing, quality control, normalisation and visualisation of single-cell RNA-seq data in R, *Bioinformatics*, 2017, **33**, 1179–1186.

47 J. Oksanen, G. Simpson, F. Blanchet, R. Kindt, P. Legendre and P. Minchin, *et al.*, vegan: Community Ecology Package, *R package version 2.6-8*, 2024.

48 D. Papciak, A. Domon, M. Zdeb, A. Skwarczynsk-Wojsa and J. Konkol, Optimization of quantitative analysis of biofilm cell from pipe materials, *Coatings*, 2021, **11**, 1286.

49 C. Wilson, R. Lukowicz, S. Merchant, H. Valquier-Flynn, J. Caballero and J. Sandoval, *et al.*, Quantitative and qualitative assessment methods for biofilm growth: a mini-review, *Res. Rev.: J. Eng. Technol.*, 2017, **6**, 4.

50 J. Swietlik and M. Magnucka, Chemical and microbiological safety of drinking water in distribution networks made of plastic pipes, *Wiley Interdiscip. Rev.: Water*, 2024, **11**, e1704.

51 S. Gurian, N. Samuel, N. Yadav and M. Krieger, *et al.*, Impact of premise plumbing design, velocity, and operational factors on microbial activity during stagnation in pipes, *AWWA Water Sci.*, 2025, **7**, e70031.

52 I. B. Gomes, M. Simões and L. C. Simões, Copper surfaces in biofilm control, *Nanomaterials*, 2020, **10**, 2491.

53 K. L. G. Learbuch, H. Smidt and P. W. J. J. van der Wielen, Influence of pipe materials on microbial community in

unchlorinated drinking water and biofilm, *Water Res.*, 2021, **194**, 116922.

54 I. B. Gomes, M. A. Pereira, L. C. Simões and M. Simões, Influence of surface materials on biofilm formation, in: *Viruses, Bacteria and Fungi in the Built Environment*, 2022, pp. 45–63.

55 A. Ren, J. Li, Z. Zhang, E. van der Mark, L. Chen and X. Li, *et al.*, Long-term influences of pipe materials on bacterial communities of matured biofilms (> 40 years' old) in drinking water distribution systems, *Fundam. Res.*, 2024, DOI: 10.1016/j.fmre.2024.05.019.

56 I. Douterelo, S. Husband and V. Loza, Dynamics of biofilm regrowth in drinking water distribution systems, *Appl. Environ. Microbiol.*, 2016, **82**, 4155–4168.

57 M. Li, X. Ma, J. Eisener, P. Pfeiffer, C. D. Ohl and C. Sun, How bulk nanobubbles are stable over a wide range of temperatures, *J. Colloid Interface Sci.*, 2021, **596**, 184–198.

58 C.-S. Chen, Y. Gao and X. Zhang, The Existence and Stability Mechanism of Bulk Nanobubbles: A Review, *Nanomaterials*, 2025, **15**(4), 314.

59 W. Xiao and G. Xu, Mass transfer of nanobubble aeration and its effect on biofilm growth: Microbial activity and structural properties, *Sci. Total Environ.*, 2020, **703**, 134976.

60 M. Ito and Y. Sugai, Nanobubbles activate anaerobic growth and metabolism of Pseudomonas aeruginosa, *Sci. Rep.*, 2021, **11**, 16858.

61 N. L. H. Tran, T. Q. Lam, P. V. Q. Duong, L. H. Doan, M. P. Vu and K. H. P. Nguyen, *et al.*, Review on the significant interactions between ultrafine gas bubbles and biological systems, *Langmuir*, 2024, **40**, 984–996.

62 H. Jung, U. Kim, G. Seo and H. C. Lee, Effect of dissolved oxygen (DO) on internal corrosion of water pipes, *Environ. Eng. Res.*, 2009, **14**, 195–199.

63 A. Lundin, Use of firefly luciferase in ATP related assays of biomass, enzymes and metabolites, *Methods Enzymol.*, 2000, **305**, 346–370.

64 Y. Ke, W. Sun, S. Liu, Y. Zhu, S. Yan and X. Chen, *et al.*, Seasonal variations of biofilm C, N and S cycling genes in a pilot-scale chlorinated drinking water distribution system, *Water Res.*, 2023, **247**, 120759.

65 S. Gholipour, Z. Shamsizadeh, W. Gwenzi and M. Nikaeen, The bacterial biofilm resistome in drinking water distribution systems: A systematic review, *Chemosphere*, 2023, **329**, 138642.

66 Y. Ma, Y. Zhang, H. Wang, G. Liu and W. T. Liu, Seasonal variations of biofilm C, N and S cycling genes in a pilot-scale drinking water distribution system, *Water Res.*, 2023, **245**, 120681.

67 X. T. Ma, M. B. Li and C. Sun, Measurement and characterization of bulk nanobubbles by nanoparticle tracking analysis method, *J. Hydrodyn.*, 2022, **34**, 1121–1133.

This journal is © The Royal Society of Chemistry 2026

Environ. Sci.: Water Res. Technol., 2026, **12**, 1264–1279 | **1279**